We are IntechOpen, the world's leading publisher of Open Access books Built by scientists, for scientists

4,800
Open access books available

122,000
International authors and editors

135M
Downloads

Our authors are among the

154
Countries delivered to

TOP 1%
most cited scientists

12.2%
Contributors from top 500 universities

CLARIVATE ANALYTICS BOOK CITATION INDEX INDEXED

WEB OF SCIENCE™

Selection of our books indexed in the Book Citation Index in Web of Science™ Core Collection (BKCI)

Interested in publishing with us?
Contact book.department@intechopen.com

Numbers displayed above are based on latest data collected.
For more information visit www.intechopen.com

Chapter

Nyquist-Like Stability Criteria for Fractional-Order Linear Dynamical Systems

Jun Zhou

Abstract

In this chapter, we propose several Nyquist-like stability criteria for linear dynamical systems that are described by fractional commensurate order linear time-invariant (FCO-LTI) state-space equations (thus endowed with fractional-order transfer functions) by means of the argument principle for complex analysis. Based on the standard Cauchy integral contour or its shifting ones, the stability conditions are necessary and sufficient, independent of any intermediate poles computation, domain transformation, and distribution investigation, which can be implemented graphically with locus plotting or numerically without any locus plotting. The proposed criteria apply to both single and multiple fractional cases as well and can be exploited in regular-order systems without any modification. Case study is included.

Keywords: fractional-order, commensurate, stability, meromorphic/holomorphic, argument principle, Cauchy integral contour

1. Introduction

Fractional-order calculus possesses a long history in pure mathematics. In recent decades, its involvements in systems, control, and engineering have attracted great attention; in the latest years, its significant extensions in various aspects of systems and control are frequently encountered [1–8]. It turns out that phenomena modeled with fractional-order calculus much more widely exist than those based on regular-order ones. It has been shown that fractional-order calculus describes real-world dynamics and behaviors more accurately than the regular-order counterparts and embraces many more analytical features and numerical properties of the observed things; indeed, many practical plants and objects are essentially fractional-order. Without exhausting the literature, typical examples include the so-called non-integer-order system of the voltage–current relation of semi-infinite lossy transmission line [9] and diffusion of the heat through a semi-infinite solid, where heat flow is equal to the half-derivative of the temperature [10].

One of the major difficulties for us to exploit the fractional-order models is the absence of solution formulas for fractional-order differential equations. Lately, lots of numerical methods for approximate solution of fractional-order derivative and integral are suggested such that fractional-order calculus can be solved numerically. As far as fractional-order systems and their control are concerned, there are mainly three schools related to fractional-order calculus in terms of system configuration:

(i) integer-order plant with fractional-order controller, (ii) fractional-order plant with integer-order controller, and (iii) fractional-order plant with fractional-order controller. The principal reason for us to bother with fractional-order controllers is that fractional-order controllers can outperform the integer-order counterparts in many aspects. For example, it has been confirmed that fractional-order PID can provide better performances and equip designers with more parametrization freedoms (due to its distributed parameter features [4, 11–13]).

An important and unavoidable problem about fractional-order systems is stability [13–15]. As is well known, stability in integer-order LTI systems is determined by the eigenvalues distribution; namely, whether or not there are eigenvalues on the close right-half complex plane. The situation changes greatly in fractional-order LTI systems, due to its specific eigenvalue distribution patterns. More precisely, on the one hand, eigenvalues of fractional-order LTI systems cannot generally be computed in analytical and closed formulas; on the other hand, stability of the fractional-order LTI systems is reflected by the eigenvalue distribution in some case-sensitive complex sectors [13, 15], rather than simply the close right-half complex plane for regular-order LTI systems. In this paper, we revisit stability analysis in fractional commensurate order LTI (FCO-LTI) systems by exploiting the complex scaling methodology, together with the well-known argument principle for complex analysis [16]. This work is inspired by the study for structural and spectral characteristics of LTI systems that is also developed by means of the argument principle [17–19]. The complex scaling technique is a powerful tool in stability analysis and stabilization for classes of linear and/or nonlinear systems; the relevant results by the author and his colleagues can be found in [20–25]. Also around fractional-order systems, the main results of this chapter are several Nyquist-like criteria for stability with necessary and sufficient conditions [26], which can be interpreted and implemented either graphically with loci plotting or numerically without loci plotting, independent of any prior pole distribution and complex/frequency-domain facts.

Outline of the paper. Section 2 reviews basic concepts and propositions about stability in FCO-LTI systems that are depicted by fractional commensurate order differential equations or state-space equations. The main results of the study are explicated in Section 3. Numerical examples are sketched in Section 4, whereas conclusions are given in Section 5.

Notations and terminologies of the paper. $\mathcal{R}$ and $\mathcal{C}$ denote the sets of all real and complex numbers, respectively. I_k denotes the $k \times k$ identity matrix, while $\mathcal{C}^+$ is the open right-half complex plane, namely, $\mathcal{C}^+ = \{s \in \mathcal{C} : \mathrm{Re}[s] > 0\}$. $(\cdot)^*$ means the conjugate transpose of a matrix $(\cdot)$. $N(\cdot)$, $N_c(\cdot)$, and $N\bar{c}(\cdot)$ stand for the net, clockwise, and counterclockwise encirclements of a closed complex curve $(\cdot)$ around the origin $(0, j0)$. By definition, $N(\cdot) = N_c(\cdot) - N\bar{c}(\cdot)$. In particular, $N(\cdot) = 0$ means that the number of clockwise encirclements of $(\cdot)$ around the origin is equal to that of counterclockwise encirclements.

2. Preliminaries and properties in FCO-LTI systems

2.1 Preliminaries to fractional-order calculus

Based on [13, 15], fractional-order calculus can be viewed as a generalization of the regular (integer-order) calculus, including integration and differentiation. The basic idea of fractional-order calculus is as old as the regular one and can be traced back to 1695 when Leibniz and L'Hôpital discussed what they termed the half-order derivative. The exact definition formula for the so-called r-order calculus was well established then by Riemann and Liouville in the form of

$$ {}_{\alpha}D_t^r f(t) = \frac{1}{\Gamma(n-r)} \frac{d^n}{dt^n} \int_{\alpha}^{t} \frac{f(\tau)}{(t-\tau)^{r-n+1}} d\tau \tag{1} $$

where $\alpha \geq 0$ and $r \geq 0$ are real numbers while $n \geq 1$ is an integer; more precisely, $n-1 \leq r < n$ and n is the smallest integer that is strictly larger than r. $\Gamma(n-r)$ is the gamma function at $n-r$; by ([16], p. 160), $\Gamma(n-r) = \int_0^{\infty} e^{-\tau} \tau^{n-r-1} d\tau$ and it is convergent for each $n-r > 0$.

Basic facts about fractional-order calculus are given as follows [13]:

- If $f(t)$ is analytical in t, then ${}_{\alpha}D_t^r f(t)$ is analytical in t and r.
- If $r \geq 0$ is an integer and $n = r+1$, then ${}_{\alpha}D_t^r f(t)$ reduces to the $(r+1)$th-order derivative of $f(t)$ with respect to t; namely, ${}_{\alpha}D_t^r f(t) = d^{r+1} f(t)/dt^{r+1}$.
- If $r = 0$ and thus $n = 1$, the definition formula for ${}_{\alpha}D_t^r f(t) = {}_{\alpha}D_t^0 f(t)$ yields the identity relation ${}_{\alpha}D_t^0 f(t) = f(t)$.
- Fractional-order differentiation and integration are linear operations. Thus

$$ {}_{\alpha}D_t^r [af(t) + bg(t)] = a\left[{}_{\alpha}D_t^r f(t) f(t)\right] + b\left[{}_{\alpha}D_t^r g(t)\right]. $$

- Under some additional assumptions about $f(t)$, the following additive index relation (or the semigroup property) holds true:

$$ {}_{\alpha}D_t^{r_1}\left[{}_{\alpha}D_t^{r_2} f(t)\right] = {}_{\alpha}D_t^{r_2}\left[{}_{\alpha}D_t^{r_1} f(t)\right] = {}_{\alpha}D_t^{r_1+r_2} f(t) $$

- If $f^{(k)}(t)\Big|_{t=\alpha} = 0$ for $k = 0, 1, \cdots, m$ with m being a positive integer, then fractional-order derivative commutes with integer-order derivative:

$$ \frac{d^m}{dt^m}\left[{}_{\alpha}D_t^r f(t)\right] = {}_{\alpha}D_t^r\left[\frac{d^m}{dt^m} f(t)\right] = {}_{\alpha}D_t^{r+m} f(t) $$

The fractional-order calculus (1) and its properties are essentially claimed in the time domain. Therefore, it is generally difficult to handle these relations directly and explicitly. To surmount such difficulties, the Laplace transform of (1) is frequently used, which is given by

$$ \mathcal{L}\left\{{}_0D_t^r f(t)\right\} = \int_0^{\infty} e^{-st} {}_0D_t^r f(t) dt = s^r F(s) - \sum_{k=0}^{n-1} s^k {}_0D_t^r f(t)\Big|_{t=0} \tag{2} $$

where $F(s) = \mathcal{L}\{f(t)\}$ and s is the Laplace transform variable. Under the assumption that the initial conditions involved are zeros, it follows that $\mathcal{L}\left\{{}_0D_t^r f(t)\right\} = s^r F(s)$. To simplify our notations, we denote ${}_0D_t^r f(t)S$ by $D_t^r f(t)$ in the following if nothing otherwise is meant.

2.2 Definition and features of FCO-LTI state-space equations

A scalar fractional-order linear time-invariant system can be described with a fractional-order state-space equation in the form of

$$ \begin{cases} D_t^r x(t) = Ax(t) + Bu(t) \\ y(t) = Cx(t) + Du(t) \end{cases} \tag{3} $$

where $x(t) = [x_1(t), \cdots, x_n(t)]^T \in \mathcal{R}^n$, $u(t) \in \mathcal{R}$, and $y(t) \in \mathcal{R}$ are the state, input, and output vectors, respectively. In accordance with $x(t)$, $u(t)$

and $y(t)$, $A \in \mathcal{R}^{n\times n}$, $B \in \mathcal{R}^{n\times 1}$, $C \in \mathcal{R}^{1\times n}$, and $D \in \mathcal{R}^{1\times 1}$ are constant matrices. We denote:

$$D_t^r x(t) =: \begin{bmatrix} D_t^{r_n} x_1(t) \\ \vdots \\ D_t^{r_1} x_n(t) \end{bmatrix} \in \mathcal{R}^n$$

For simplicity, we employ r to stand for the fractional-order indices set $\{r_n, \cdots, r_1\}$ with $0 \le r_i < 1$ with a little abuse of notations. The corresponding transfer function follows as

$$G(s) = C(\operatorname{diag}[s^{r_n}, \cdots, , s^{r_1}] - A)^{-1}B + D = \frac{b_m s^{\beta_m} + b_{m-1}s^{\beta_{m-1}} + \cdots + b_1 s^{\beta_1}}{a_n s^{\alpha_n} + a_{n-1}s^{\alpha_{n-1}} + \cdots + a_1 s^{\alpha_1}} \quad (4)$$

which is the fractional-order transfer function defined from $U(s)$ to $Y(s)$. In (4), $\operatorname{diag}[s^{r_n}, \cdots, s^{r_1}] \in \mathcal{C}^{n\times n}$ stands for a diagonal matrix. Also, $a_k\,(k = 1, \cdots, n)$ and $b_k\,(k = 1, \cdots, m)$ are constants, while $\alpha_k\,(k = 1, \cdots, n)$ and $\beta_k\,(k = 1, \cdots, m)$ are nonnegative real numbers satisfying

$$\begin{cases} \alpha_n > \alpha_{n-1} > \cdots > \alpha_1 \ge 0 \\ \beta_m > \beta_{m-1} > \cdots > \beta_1 \ge 0 \end{cases}$$

In the following, the fractional-order polynomial

$$\Delta(s, r_n, \cdots, r_1) = \det(\operatorname{diag}[s^{r_n}, \cdots, s^{r_1}] - A) = a_n s^{\alpha_n} + a_{n-1}s^{\alpha_{n-1}} + \cdots + a_1 s^{\alpha_1} \quad (5)$$

is called the characteristic polynomial of the state-space equation (3).

We note by complex analysis ([16], p. 100) that s^α is well-defined and satisfies

$$s^\alpha = e^{\alpha \log s}, \quad \forall s \in \mathcal{C}\backslash\{0\}, \forall \alpha \in \mathcal{C} \quad (6)$$

where $\log s$ is the principal branch of the complex logarithm of s or the principal sheet of the Riemann surface in the sense of $-\pi < \arg s \le \pi$. In view of (6), we see that $\Delta(s, r_n, \cdots, r_1)$ as fractional-order polynomial and $G(s)$ as fractional-order fraction are well-defined only on $\mathcal{C}\backslash\{0\}$ for all $r_i, \alpha_i, \beta_i \in \mathcal{C}$, whenever at least one of $\{r_i\}$, $\{\alpha_i\}$, and $\{\beta_i\}$ is a fraction number. Both are well-defined on the whole complex plane $\mathcal{C}$, if all $\{r_i\}$, $\{\alpha_i\}$, and $\{\beta_i\}$ are integers.

Bearing (6) in mind, our questions are (i) under what conditions $\Delta(s, r_n, \cdots, r_0)$ is holomorphic and has only isolated zeros and (ii) under what conditions $G(s)$ is meromorphic and has only isolated zeros and poles?

To address (i), let us return to (6) and observe for any $s \in \mathcal{C}\backslash 0$ and $\alpha \in \mathcal{C}$ that

$$\begin{aligned} \frac{d}{ds}s^\alpha &= \frac{d}{ds}e^{\alpha \log s} = \frac{d}{ds}\left[\sum_{k=0}^{\infty}\frac{1}{k!}(\alpha \log s)^k\right] \\ &= \sum_{k=0}^{\infty}\frac{1}{k!}\frac{d}{ds}(\alpha \log s)^k \\ &= \sum_{k=0}^{\infty}\frac{1}{(k-1)!}(\alpha \log s)^{k-1}\alpha\frac{d}{ds}\log s \\ &= \alpha\sum_{k=1}^{\infty}\frac{1}{(k-1)!}(\alpha \log s)^{k-1}s^{-1} \\ &= \alpha e^{\alpha \log s}s^{-1} = \alpha e^{\alpha \log s}e^{-\log s} \\ &= \alpha e^{(\alpha-1)\log s} = \alpha\left(e^{\log s}\right)^{\alpha-1} = \alpha s^{\alpha-1} \end{aligned}$$

where we have used $\frac{d}{ds}\log s = s^{-1}$ for any $s \neq 0$ (see [27], p. 36). The deductions above actually say by the definition ([16], p. 8) that each term in $\Delta(s, r_n, \cdots, r_1)$ on $\mathcal{C}\backslash\{0\}$ is holomorphic. Thus, $\Delta(s, r_n, \cdots, r_1)$ is holomorphic on $\mathcal{C}\backslash\{0\}$.

To see under what conditions $\Delta(s, r_n, \cdots, r_1)$ (respectively, $G(s)$) possesses only isolated zeros and poles, let us assume that there exists $0 < r \leq 1$ such that

$$\begin{cases} \alpha_n = k_n r > \alpha_{n-1} = k_{n-1} r > \cdots > \alpha_1 = k_1 r \\ \beta_m = l_m r > \beta_{m-1} = l_{m-1} r > \cdots > \beta_1 = l_1 r \end{cases} \tag{7}$$

where $k_n > k_{n-1} > \cdots > k_1 \geq 0$, $l_m > l_{m-1} > \cdots > l_1 \geq 0$, and $k_n \geq l_m$ are integers. Then, if we set $z = s^r$, then $G(s)$ and $\Delta(s, r_n, \cdots, r_1)$ can be re-expressed as

$$\begin{cases} G(z, r) = \dfrac{b_m z^{l_m} + b_{m-1} z^{l_{m-1}} + \cdots + b_1 z^{l_1}}{a_n z^{k_n} + a_{n-1} z^{k_{n-1}} + \cdots + a_1 z^{k_1}} \\ \Delta(z, r) = a_n z^{k_n} + a_{n-1} z^{k_{n-1}} + \cdots + a_1 z^{k_1} \end{cases} \tag{8}$$

Obviously, $G(z, r)$ is a so-called rational function on the z-complex plane and possesses only finitely many isolated zeros and poles. More precisely, $G(z, r)$ is a special meromorphic function that is determined up to a multiplicative constant by prescribing the locations and multiplicities of its zeros and poles ([16], p. 87); or equivalently it is in the form of a complex fraction with regular-order polynomials as its nominator and denominator. Also, $\Delta(z, r)$ is a regular-order polynomial that is holomorphic on the whole z-complex plane and has finitely many isolated zeros. Thus, $G(z, r)$ and $\Delta(z, r)$ can be written in the form of

$$\begin{cases} G(z, r) = \dfrac{b_m \prod_l (z + z_l)^{\mu_l}}{a_n \prod_k (z + p_k)^{\nu_k}} \\ \Delta(z, r) = a_n \prod_k (z + p_k)^{\nu_k} \end{cases} \tag{9}$$

Under the assumption that (7) and suppose that $G(z, r)$ and $\Delta(z, r)$ have no zero, zeros, and zero singularities, it holds that $z_l \neq 0, p_k \neq 0 \in \mathcal{C}$. In addition, $\mu_l \geq 1, \nu_k \geq 1$ are integers such that $\sum_l \mu_l = l_m$ and $\sum_k \nu_k = k_n$.

Based on (6) and (9), the s-domain relationships can be rewritten by

$$\begin{cases} G(s) = \dfrac{b_m \prod_l (s^r + z_l)^{\mu_l}}{a_n \prod_k (s^r + p_k)^{\nu_k}} \\ \Delta(s, r_n, \cdots, r_1) = a_n \prod_k (s^r + p_k)^{\nu_k} \end{cases} \tag{10}$$

By (10), it is not hard to see that $G(s) = 0$ as $s^r \to z_l$ (or equivalently by (6), $s \to \exp\left\{\frac{\log z_l}{r}\right\}$) and $|G(s)| \to \infty$ as $s^r \to p_k$ (or equivalently, $s \to \exp\left\{\frac{\log p_k}{r}\right\}$). The latter says specifically by Corollary 3.2 of [16] that $s = \exp\{\log p_k / r\}$ is a pole of $G(s)$. Then, $G(s)$ is holomorphic on $\mathcal{C}\backslash\{\exp\{\log p_k / r\}\}_k$ and has only finitely many isolated zeros and poles. It follows by ([16], pp. 86–87) that $G(s)$ is meromorphic on $\mathcal{C}\backslash\{0\}$. Confined to the discussion of this paper, $G(s)$ may or may not be rational.

In the sequel, when the assumption (7) is true and $\Delta(z, r)$ and $G(z, r)$ have no zeros and poles at the origin, then $\Delta(s, r_n, \cdots, r_1)$ and $G(s)$ are well-defined on $\mathcal{C}\backslash\{0\}$ with respect to fractional commensurate order r. Only fractional commensurate systems are considered in this study.

2.3 Closed-loop configuration with FCO-LTI systems

Consider the feedback system illustrated in **Figure 1**, in which we denote by Σ_G and Σ_H, respectively, an FCO-LTI plant and an FCO-LTI feedback subsystem that possess the following fractional-order state-space equations.

$$\Sigma_G : \begin{cases} D_t^r x = Ax + Be \\ y = Cx + De \end{cases}, \quad \Sigma_H : \begin{cases} D_t^q \zeta = \Lambda\zeta + \Gamma\mu \\ \eta = \Theta\zeta + \Pi\mu \end{cases} \tag{11}$$

where $A \in \mathcal{R}^{n\times n}$, $B \in \mathcal{R}^{n\times m}$, $C \in \mathcal{R}^{l\times n}$, and $D \in \mathcal{R}^{l\times m}$, respectively, are constant matrices, while $\Lambda \in \mathcal{R}^{p\times p}$, $\Gamma \in \mathcal{R}^{p\times l}$, $\Theta \in \mathcal{R}^{m\times p}$, and $\Pi \in \mathcal{R}^{m\times l}$ are constant.

Fractional-order transfer functions for Σ_G and Σ_H are given as follows:

$$\begin{cases} G(s) = C(\,\mathrm{diag}\,[s^{r_n}, \cdots, , s^{r_1}] - A)^{-1}B + D \\ \quad =: C(I_n(s,r) - A)^{-1}B + D =: \hat{G}(s) + D \\ \quad =: \dfrac{C\,\mathrm{adj}\,(I_n(s,r) - A)B + \det(I_n(s,r) - A)D}{\det(I_n(s,r) - A)} \\ \quad =: \breve{G}(s)/\det(I_n(s,r) - A) \\ H(s) = \Theta(\,\mathrm{diag}\,[s^{q_p}, \cdots, , s^{q_1}] - \Lambda)^{-1}\Gamma + \Pi \\ \quad =: \Theta\big(I_p(s,q) - \Lambda\big)^{-1}\Gamma + \Pi =: \hat{H}(s) + \Pi \\ \quad =: \dfrac{\Theta\ \ \mathrm{adj}\,\big(I_p(s,q) - \Lambda\big)\Gamma + \det\big(I_p(s,q) - \Lambda\big)\Pi}{\det\big(I_p(s,q) - \Lambda\big)} \\ \quad =: \breve{H}(s)/\det\big(I_p(s,q) - \Lambda\big) \end{cases} \tag{12}$$

where $\hat{G}(s)$, $\hat{H}(s)$, $\breve{G}(s)$, and $\breve{H}(s)$ are obvious and $adj\,(\cdot)$ is the adjoint. Also

$$I_n(s,r) = \mathrm{diag}\,[s^{r_n}, \cdots, s^{r_1}], \quad I_p(s,q) = \mathrm{diag}\,[s^{q_p}, \cdots, s^{q_1}]$$

Now we construct the state-space equations for the open- and closed-loop systems of **Figure 1**. The open-loop system can be expressed by the fractional-order state-space equation:

$$\Sigma_O : \begin{cases} \begin{bmatrix} D_t^r x \\ D_t^q \zeta \end{bmatrix} = \begin{bmatrix} A & 0 \\ \Gamma C & \Lambda \end{bmatrix} \begin{bmatrix} x \\ \zeta \end{bmatrix} + \begin{bmatrix} B \\ \Gamma D \end{bmatrix} u \\ \eta = [\Pi C \ \ \Theta] \begin{bmatrix} x \\ \zeta \end{bmatrix} + \Pi D u \end{cases} \tag{13}$$

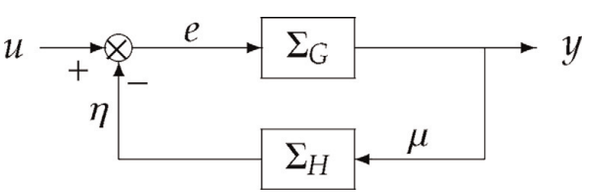

Figure 1.
FCO-LTI feedback configuration.

In the closed-loop system, we can write the closed-loop state-space equation as

$$\Sigma_C : \begin{cases} \begin{bmatrix} D_t^r x \\ D_t^q \zeta \end{bmatrix} = \begin{bmatrix} A - B\Xi\Pi C & -B\Xi\Theta \\ \Gamma C - \Gamma D\Xi\Pi C & \Lambda - \Gamma D\Xi\Theta \end{bmatrix} \begin{bmatrix} x \\ \zeta \end{bmatrix} + \begin{bmatrix} B\Xi \\ \Gamma D\Xi \end{bmatrix} u \\ \eta = \begin{bmatrix} \Xi\Pi C & \Xi\Theta \end{bmatrix} \begin{bmatrix} x \\ \zeta \end{bmatrix} + \Pi D\Xi u \end{cases} \tag{14}$$

where $\Xi = (I_m + \Pi D)^{-1}$. To explicate the Nyquist approach, we begin with the conventional return difference equation in the feedback configuration Σ_C.

By definition, the characteristic polynomial for the closed-loop system Σ_C is

$$\begin{aligned} \Delta_C(s,r,q) &:= \det\left(\begin{bmatrix} I_n(s,r) & 0 \\ 0 & I_p(s,q) \end{bmatrix} - \begin{bmatrix} A - B\Xi\Pi C & -B\Xi\Theta \\ \Gamma C - \Gamma D\Xi\Pi C & \Lambda - \Gamma D\Xi\Theta \end{bmatrix} \right) \\ &= \det\left(\begin{bmatrix} I_n(s,r) - A & 0 \\ -\Gamma C & I_p(s,q) - \Lambda \end{bmatrix} \right) \\ &\cdot \det\left(I_{n+p} + \begin{bmatrix} I_n(s,r) - A & 0 \\ -\Gamma C & I_p(s,q) - \Lambda \end{bmatrix}^{-1} \begin{bmatrix} B\Xi\Pi C & B\Xi\Theta \\ \Gamma D\Xi\Pi C & \Gamma D\Xi\Theta \end{bmatrix} \right) \\ &= \Delta_O(s,r,q) \det\left(I_{n+p} + \begin{bmatrix} I_n(s,r) - A & 0 \\ -\Gamma C & I_p(s,q) - \Lambda \end{bmatrix}^{-1} \begin{bmatrix} B\Xi\Pi C & B\Xi\Theta \\ \Gamma D\Xi\Pi C & \Gamma D\Xi\Theta \end{bmatrix} \right) \end{aligned} \tag{15}$$

where $\det(\cdot)$ means the determinant of $(\cdot)$ and

$$\begin{aligned} \Delta_O(s,r,q) &:= \det\left(\begin{bmatrix} I_n(s,r) - A & 0 \\ -\Gamma C & I_p(s,q) - \Lambda \end{bmatrix} \right) \\ &= \det(I_n(s,r) - A) \det\big(I_p(s,q) - \Lambda\big) = \Delta_G(s,r)\Delta_H(s,q) \end{aligned} \tag{16}$$

with $\Delta_G(s,r) = \det(I_n(s,r) - A)$ and $\Delta_H(s,q) = \det\big(I_p(s,q) - \Lambda\big)$. Clearly, $\Delta_O(s,r,q)$ is the characteristic polynomial for Σ_O, while $\Delta_G(s,r)$ and $\Delta_H(s,q)$ are the characteristic polynomials for the subsystems Σ_G and Σ_H, respectively, in the feedback configuration of **Figure 1**.

Let us return to (15) and continue to observe that

$$\begin{aligned} &\Delta_C(s,r,q) \\ &= \Delta_O(s,r,q) \det\left(I_{n+p} + \begin{bmatrix} (I_n(s,r) - A)^{-1} & 0 \\ \big(I_p(s,q) - \Lambda\big)^{-1} \Gamma C (I_n(s,r) - A)^{-1} & \big(I_p(s,q) - \Lambda\big)^{-1} \end{bmatrix} \right. \\ &\left. \cdot \begin{bmatrix} B & 0 \\ 0 & \Gamma \end{bmatrix} \begin{bmatrix} \Xi\Pi & \Xi \\ D\Xi\Pi & D\Xi \end{bmatrix} \begin{bmatrix} C & 0 \\ 0 & \Theta \end{bmatrix} \right) \\ &= \Delta_O(s,r,q) \det\Big(I_{l+m} \\ &+ \begin{bmatrix} C & 0 \\ 0 & \Theta \end{bmatrix} \begin{bmatrix} (I_n(s,r) - A)^{-1} & 0 \\ \big(I_p(s,q) - \Lambda\big)^{-1} \Gamma C (I_n(s,r) - A)^{-1} & \big(I_p(s,q) - \Lambda\big)^{-1} \end{bmatrix} \end{aligned}$$

$$\cdot \begin{bmatrix} B & 0 \\ 0 & \Gamma \end{bmatrix} \begin{bmatrix} \Xi\Pi & \Xi \\ D\Xi\Pi & D\Xi \end{bmatrix} \Bigg)$$

$$= \Delta_O(s,r,q)\det\left(I_{l+m} + \begin{bmatrix} \hat{G}(s) & 0 \\ \hat{H}(s)\hat{G}(s), & \hat{H}(s) \end{bmatrix} \begin{bmatrix} \Xi\Pi & \Xi \\ D\Xi\Pi & D\Xi \end{bmatrix} \right)$$

$$= \Delta_O(s,r,q)\det\left(\begin{bmatrix} I_m + \Pi\hat{G}(s)\Xi & \Pi\hat{G}(s)\Xi \\ \hat{H}(s)G(s)\Xi, & I_m + \hat{H}(s)G(s)\Xi \end{bmatrix} \right)$$

$$= \Delta_O(s,r,q)\det\left(\begin{bmatrix} I_m & \Pi\hat{G}(s)\Xi \\ -I_m & I_m + \hat{H}(s)G(s)\Xi \end{bmatrix} \right)$$

$$= \Delta_O(s,r,q)\det\left(\begin{bmatrix} I_m & \Pi\hat{G}(s)\Xi \\ 0 & I_m + \hat{H}(s)G(s)\Xi + \Pi\hat{G}(s)\Xi \end{bmatrix} \right)$$

$$= \Delta_O(s,r,q)\det\Big(I_m + \hat{H}(s)G(s)\Xi + \Pi\hat{G}(s)\Xi \Big)$$

$$= \Delta_O(s,r,q)\det(\Xi)\det\Big(I_m + \Pi D + \hat{H}(s)G(s) + \Pi\hat{G}(s) \Big)$$

$$= \Delta_O(s,r,q)\det(\Xi)\det(I_m + H(s)G(s)) \tag{17}$$

In deriving (17), the determinant equivalence $\det(I_1 + XY) = \det(I_2 + YX)$ is repeatedly used, where X and Y are matrices of compatible dimensions and I_1 and I_2 are identities of appropriate dimensions. By (17), we have

$$\frac{\Delta_C(s,r,q)}{\Delta_O(s,r,q)} = \frac{\Delta_C(s,r,q)}{\Delta_G(s,r)\Delta_H(s,q)} = \frac{\det(I_m + H(s)G(s))}{\det(I_m + \Pi D)} \tag{18}$$

which is nothing but the return difference relationship for the fractional-order feedback system Σ_C. By the definitions, it is clear that $\Delta_O(s,r,q)$, $\Delta_O(s,r,q)$, $\Delta_G(s,r)$, and $\Delta_H(s,q)$ are all fractional-order. It is based on (18) that Nyquist-like criteria will be worked out. However, in order to get rid of any open-loop structure and spectrum, let us instead work with

$$\Delta_C(s,r,q) = \Delta_G(s,r)\Delta_H(s,q)\frac{\det(I_m + H(s)G(s))}{\det(I_m + \Pi D)} \tag{19}$$

Remark 1. Recalling our discussion in Section 2.2 and assuming that there exists a number $0 < \rho \leq 1$ such that Σ_G and Σ_H are fractionally commensurate with respect to the same commensurate order ρ, it follows that $G(s)$ and $H(s)$ are meromorphic on $\mathcal{C}\backslash\{0\}$, while $\Delta_C(s,r,q)$, $\Delta_G(s,r)$, and $\Delta_H(s,q)$ are holomorphic on the whole complex plane. These complex functional facts will play a key role for us to apply the argument principle to (18) as well as (19).

3. Main results

3.1 Nyquist contours in the z-/s-domains

As another preparation for stability analysis in fractional-order systems by means of the argument principle for meromorphic functions, we need to choose appropriate Nyquist contours.

Firstly, the simply closed curve defined on the z-domain as illustrated by the dashed-line in **Figure 2** is the standard contour for a Nyquist-like stability criterion in terms of $\Delta(z, r)$. The contour portions of $\mathcal{N}_z$ along the two slopes actually overlap the slope lines. Clearly, the contour $\mathcal{N}_z$ is actually the boundary of the sector region encircled by the dashed-line. The radiuses of the two arcs in the sector are sufficiently small and large, respectively, or simply $\gamma \to 0$ and $R \to \infty$. The sector is symmetric with respect to the real axis, whose half angle is $\frac{\pi}{2}r$.

Secondly, the simply closed curve defined on the s-domain as illustrated by **Figure 3** presents the standard contour used for a Nyquist-like stability criterion in terms of $\Delta(s, r_n, \cdots, r_1)$. Again the contour is plotted with dashed-lines; in particular, the contour portion along the imaginary axis is actually overlapping the imaginary axis. More precisely, $\mathcal{N}_s$ is the boundary of the open right-half complex plane $\mathcal{C}^+ = \{s \in \mathcal{C} : \mathrm{Re}(s) > 0\}$ in the sense that

$$\mathcal{N}_s \cup \mathcal{C}^+ = \{s \in \mathcal{C} : \mathrm{Re}(s) \geq 0\}, \quad \mathrm{Int}(\mathcal{N}_s) = \mathcal{C}^+$$

where $\mathrm{I}nt(\cdot)$ denotes the interior of a closed set. Similar to the contour $\mathcal{N}_z$, the radiuses of the two half-circles in $\mathcal{N}_s$ are sufficiently small and large, respectively, namely, $\gamma \to 0$ and $R \to \infty$.

Remarks about the contours $\mathcal{N}_z$ and $\mathcal{N}_s$:

• In both cases, the origin of the complex plane is excluded from the contours themselves and their interiors. The reason for these specific contours is that $G(s)$ and $\Delta(s, r_n, \cdots, r_1)$ (respectively, $G(z, r)$ and $\Delta(z, r)$) are well-defined merely on $\mathcal{C}\backslash\{0\}$ due to the relation (6) and $z = s^r$.

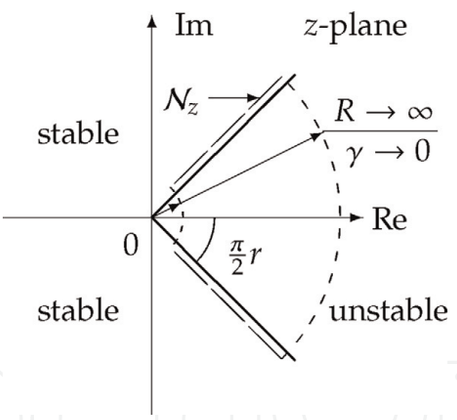

Figure 2.
The standard z-domain contour $\mathcal{N}_z$.

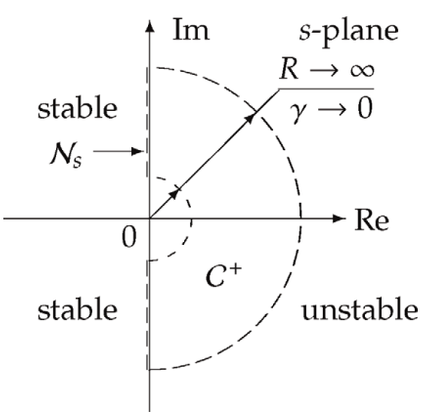

Figure 3.
The standard s-domain contour $\mathcal{N}_s$.

• One might suggest that in order to detour the origin, the small arc in $\mathcal{N}_z$ and the small half-circle in $\mathcal{N}_s$ can also be taken from the left-hand side around the origin so that possible sufficiency deficiency in the subsequent stability conditions can be dropped. In fact, if the origin is in the interior of $\mathcal{N}_s$, $G(s)$ and $\Delta(s, r_n, \cdots, r_1)$ have no definition at the origin. Therefore, the argument principle does not apply rigorously.

3.2 Stability conditions related to FCO-LTI systems

Stability conditions in terms of the zeros distribution of $\Delta(s, r_n, \cdots, r_1) = 0$ and that of $\Delta(z, r) = 0$ are given by the following proposition [13, 15].

Proposition 1. Consider the fractionally commensurate system with commensurate order $0 < r \leq 1$ defined by the fractional-order differential equation (1) or the fractional-order state-space equation (3). The system is stable if and only if all the zeros of $\Delta(s, r_n, \cdots, r_1) = 0$, denoted by $\{s_k\}_k$, have negative real parts or all the zeros of $\Delta(z, r) = 0$, denoted by $\{z_l\}_l$, satisfy

$$|\operatorname{Arg}(z_l)| > \frac{\pi}{2} r, \quad \forall z_l \tag{20}$$

where $Arg(\cdot)$ is the principal branch argument of $(\cdot)$ on the Riemann surface.

3.3 Stability criterion in FCO-LTI systems

In what follows, a fractional-order polynomial $\beta(s, r)$ is said to be commensurately Hurwitz if $\beta(s, r)$ is fractionally commensurate order r with some $0 < r \leq 1$ in the sense that all the roots of $\beta(s, r) = 0$ possess negative real parts. More specifically, we write

$$\beta(s, r) = c_p s^{r l_p} + c_{p-1} s^{r l_{p-1}} + \cdots + c_1 e^{r l_1}$$

where $l_p > l_{p-1} > \cdots > l_1 \geq 0$ are integers and $\operatorname{Re}(s) < 0$ for any $\beta(s, r) = 0$. It is straightforward to see by definition that a fractionally commensurate order Hurwitz polynomial must be holomorphic on the whole complex plane.

Theorem 1. Consider the fractional-order system with commensurate order $0 < r \leq 1$ defined by the differential equation (1) or the state-space equation (3). The concerned system is stable if and only if for any $\gamma > 0$ sufficiently small and $R > 0$ sufficiently large, any prescribed commensurate order Hurwitz polynomial $\beta(s, r)$, the stability locus

$$f(s, \beta(s, r))\Big|_{s \in \mathcal{N}_s} =: \frac{\Delta(s, r_n, \cdots, r_1)}{\beta(s, r)}\Big|_{s \in \mathcal{N}_s} \tag{21}$$

vanishes nowhere over $\mathcal{N}_s$, namely, $f(s, \beta(s, r)) \neq 0$ for all $s \in \mathcal{N}_s$; and the number of its clockwise encirclement around the origin is equal to that of its counterclockwise ones, namely,

$$N\left(f(s, \beta(s, r)|_{s \in \mathcal{N}_s}\right) = N_c\left(f(s, \beta(s, r))\Big|_{s \in \mathcal{N}_s}\right) - N_{\bar{c}}\left(f(s, \beta(s, r))\Big|_{s \in \mathcal{N}_s}\right) = 0$$

In the above, the clockwise/counterclockwise orientation of $f(s, \beta(s, r))|_{s \in \mathcal{N}_s}$ can be self-defined.

Proof of Theorem 1. By introducing any fractional-order commensurately Hurwitz polynomial $\beta(s,r)$ into $\Delta(s,r_n,\cdots,r_1)$, we obtain

$$\frac{\Delta(s,r_n,\cdots,r_1)}{\beta(s,r)} = f(s,\beta(s,r)) \tag{22}$$

Under the given assumption about the concerned characteristic polynomial and the fact that $\beta(s,r)$ is holomorphic, we can assert that $f(s,\beta(s,r))$ is well-defined in the sense that it is meromorphic and without singularities at the origin. This says in particular that the argument principle applies to (22) as long as $f(s,\beta(s,r)) \neq 0$ over $s \in \mathcal{N}_s$. Apparently, Eq. (22) holds even if there are any factor cancelations between $\Delta(s,r_n,\cdots,r_1)$ and $\beta(s,r)$. This says that all unstable poles in $Int(\mathcal{N}_s) \cup \mathcal{N}_s$, if any, remain in the left-hand side of (22).

Bearing these facts in mind, let us apply the argument principle to (22) counterclockwisely with $\mathcal{N}_s$ being the Cauchy integral contour, and then the desired assertion in terms of (25) follows.

More precisely, since $f(s,\beta(s,r))|_{s\in\mathcal{N}_s}$ vanishes nowhere over $s \in \mathcal{N}_s$, we conclude readily that

$$N_z(\Delta(s,r_n,\cdots,r_1)) - N_z(\beta(s,r)) = N\left(f(s,\beta(s,r))|_{s\in\mathcal{N}_s}\right) \tag{23}$$

where $N_z(\cdot)$ denotes the zero number of $(\cdot)$ in $\mathrm{Int}(\mathcal{N}_s) \cup \mathcal{N}_s$ and $N(\cdot)$ denotes the net number of the locus encirclements around the origin.

Note that all the roots of $\beta(s,r)$ are beyond $\mathrm{Int}(\mathcal{N}_s)$. It follows that $N(\beta(s,r)) = 0$. Together with $N(\cdot) = N_c(\cdot) - N_{\bar{c}}(\cdot)$, it follows by (17) that

$$N_z(\Delta(s,r_n,\cdots,r_1)) = N_c\left(f(s,\beta(s,r))|_{s\in C_\gamma}\right) - N_{\bar{c}}\left(f(s,\beta(s,r))|_{s\in C_\gamma}\right)$$

The above equation says that $N_z(\Delta(s,r_n,\cdots,r_1)) = 0$ if and only if $N\left(f(s,\beta(s,r))|_{s\in C_\gamma}\right) = 0$. The desired results are verified if we mention that $N_z(\Delta(s,r_n,\cdots,r_1)) = 0$ is equivalent to the assertion that $\Delta(s,r_n,\cdots,r_1) = 0$ has no roots in $Int(\mathcal{N}_s) \cup \mathcal{N}_s$. This says exactly that $\Delta(s,r_n,\cdots,r_1) = 0$ has no roots in $Int(\mathcal{N}_s) \cup \mathcal{N}_s$, and thus the concerned system is stable.

Several remarks about Theorem 1.

• Theorem 1 is independent of the contour and locus orientations; or the locus orientations can be alternatively defined after the locus is already drawn. The fractionally commensurate Hurwitz polynomial $\beta(s,r)$ can be arbitrarily prescribed so that no existence issues exist. In addition, the stability locus is not unique. The polynomial $\beta(s,r)$ actually provides us additional freedom in frequency-domain analysis and synthesis.

• When the stability locus with respect to the infinite portion of $\mathcal{N}_s$ is concerned, it is most appropriate to let the commensurate degree of $\beta(s,r)$, namely, c-deg$(\beta(s,r)) = l_p$, satisfy $l_p = k_n$, although $\beta(s,r)$ can be arbitrary as long as it is fractionally commensurate Hurwitz. For example, in the sense of (25), if c-deg$(\beta(s,r)) > k_n$, the stability locus approaches the origin $(0,j0)$ as $s \to \infty$. It may be graphically hard to discern possible encirclements around $(0,j0)$; if c-deg$(\beta(s,r)) < k_n$, the stability locus contains portions that are plotted infinitely far from $(0,j0)$. When c-deg$(\beta(s,r)) = k_n$ and let $\beta(s,r) = L\beta'(s,r)$ with $L > 0$ be constant and $\beta'(s,r)$ monic, it follows from (25) that

$$\lim_{s\to\infty} f(s,\beta(s,r)) = \lim_{s\to\infty} \frac{\Delta(s,r_n,\cdots,r_1)}{L\beta'(s,r)} = 1/L < \infty \tag{24}$$

Since $f(s,\beta(s,r))$ is continuous in s, (27) says that $|f(s,\beta(s,r))| \le M$ over $s \in \mathcal{N}_s$ for some $0 < M < \infty$ and $f(s,\beta(s,r))|_{s\in\mathcal{N}_s}$ can be plotted in a bounded region around the origin. Thus, no prior frequency sweep is needed when dealing with the stability locus (25).

• Each and all the conditions in Theorem 1 can be implemented only by numerically integrating $\angle f(s,\beta(s,r))$ for computing the argument incremental $\nabla\angle f(s,\beta(s,r))$ along the Cauchy integral contour $\mathcal{N}_s$, and then checking if $\nabla\angle f(s,\beta(s,r))/2\pi = 0$ holds. In this way, numerically implementing Theorem 1 entails no graphical locus plotting. This is also the case for the following results.

• The clockwise/counterclockwise orientation of $f(s,\beta(s,r))|_{s\in\mathcal{N}_s}$ can be self-defined. This is also the case in all the subsequent results.

Next, a regular-order polynomial $\alpha(z,r)$ is said to be πr-sector Hurwitz if all the roots of $\alpha(z,r) = 0$ satisfy (20). More specifically, we write

$$\alpha(z,r) = c_p z^{l_p} + c_{p-1} z^{l_{p-1}} + \cdots + c_1 z^{l_1}$$

where $l_p > l_{p-1} > \cdots > l_1 \ge 0$ are integers and $\mathrm{Arg}(z) < 0$ for any $\alpha(z,r) = 0$. It is easy to see that a πr-sector Hurwitz polynomial is holomorphic.

Theorem 2. Consider the fractional-order system with commensurate order $0 < r \le 1$ of the differential equation (1) or the state-space equation (3). The system is stable if and only if for any $\gamma > 0$ small and $R > 0$ large sufficiently, any prescribed πr-sector Hurwitz polynomial $\alpha(z,r)$, the stability locus

$$g(z,\alpha(z,r))\Big|_{z\in\mathcal{N}_z} =: \frac{\Delta(z,r)}{\alpha(z,r)}\Big|_{z\in\mathcal{N}_z} \tag{25}$$

vanishes nowhere over $\mathcal{N}_z$, namely, $g(z,\alpha(z,r)) \ne 0$ for all $z \in \mathcal{N}_z$; and the number of its clockwise encirclement around the origin is equal to that of its counterclockwise ones, namely, $N\left(g(z,\alpha(z,r)|_{z\in\mathcal{N}_z}\right) = 0$.

Proof of Theorem 2. Repeating those for Theorem 1 but in terms of $g(z,\alpha(z,r))$ rather with $f(s,\beta(s,r))$, while the contour $\mathcal{N}_s$ is replaced with $\mathcal{N}_z$.

Remark 2. The proof arguments can also be understood by using the transformation $z = s^r$ to (22) and then applying the argument principle to the resulting z-domain relationship. Note that $z = s^r$ is holomorphic on $C\backslash\{0\}$. The angle preserving property ([16], pp. 255–256) leads immediately that the stability conditions of Theorem 2 are equivalent to those of Theorem 1.

3.4 Stability criteria for closed-loop FCO-LTI systems

Based on the return difference equation (31) claimed in the feedback configuration of **Figure 1**, together with the argument principle, the following s-domain criterion follows readily.

Theorem 3. Consider the feedback system as in **Figure 1** with the fractional-order subsystems Σ_G and Σ_H defined in (22). Assume that both subsystems are fractionally commensurate with respect to a same commensurate order $0 < \rho \le 1$.

Then, the closed-loop system is stable if and only if for any s-domain contour $\mathcal{N}_s - \epsilon$ with $R > 0$ sufficiently large and $\gamma > 0$, $\epsilon \geq 0$ sufficiently small, any prescribed commensurate order Hurwitz polynomial $\beta(s, r)$; the locus

$$f_C(s, \beta(s,\rho))\Big|_{s\in\mathcal{N}_s-\epsilon} =: \frac{\Delta_G(s,\rho)\Delta_H(s,\rho)}{\beta(s,\rho)} \frac{\det(I_m + H(s)G(s))}{\det(I_m + \Xi D)}\Big|_{s\in\mathcal{N}_s-\epsilon} \tag{26}$$

satisfies: (i) $f_C(s, \beta(s,\rho)) \neq 0$ for all $s \in \mathcal{N}_s - \epsilon$; (ii) $N\left(f_C(s, \beta(s,\rho))\Big|_{s\in\mathcal{N}_s-\epsilon}\right) = 0$. Here, $\mathcal{N}_s - \epsilon$ stands for the contour by shifting $\mathcal{N}_s$ to its left with distance ϵ.

Proof of Theorem 3. Under the given assumptions, the return difference equation (19) is well-defined on $\mathcal{N}_s - \epsilon$ and $\mathrm{Int}(\mathcal{N}_s - \epsilon)$. Then, applying the argument principle to (19) and repeating some arguments similar to those in the proof for Theorem 1, the desired results follow readily.

To complete the proof, it remains to only show why we must work with the contour $\mathcal{N}_s - \epsilon$ in general, rather than the standard contour $\mathcal{N}_s$ itself directly. To see this, we notice that the shifting factor $\epsilon \geq 0$ is introduced for detouring possible open-loop zeros and poles on the imaginary axis but excluding the origin. Since all zeros and poles, if any, are isolated, $\epsilon \geq 0$ is always available. Furthermore, we have by (12) that

$$\begin{aligned}
&\Delta_G(s,\rho)\Delta_H(s,\rho)\frac{\det(I_m + H(s)G(s))}{\det(I_m + \Xi D)} \\
&= \Delta_G(s,\rho)\Delta_H(s,\rho)\frac{\det\left(\Delta_G(s,\rho)\Delta_H(s,\rho)I_m + \breve{H}(s)\breve{G}(s)\right)}{\Delta_G^m(s,\rho)\Delta_H^m(s,\rho)\det(I_m + \Xi D)}
\end{aligned}$$

which says clearly that if there are imaginary zeros of $\Delta_G(s,\rho)\Delta_H(s,\rho)$, then factor cancelation will happen between $\Delta_G(s,\rho)\Delta_H(s,\rho)$ and $\det(I_m + H(s)G(s))$. Such factor cancelation, if any, can be revealed analytically as in the above algebras, whereas it does bring us trouble in numerically computing the locus (obviously, numerical computation cannot reflect any existence of factor cancelation rigorously). Consequently, when the standard contour $\mathcal{N}_s$ is adopted, if there do exist imaginary open-loop poles, the corresponding stability locus cannot be well-defined with respect to $\mathcal{N}_s$. When this happens, one need to know the exact positions of imaginary zeros and/or poles and modify the contour accordingly to detour them before computing the locus; in other words, working with $\mathcal{N}_s$ brings sufficiency deficiency when imaginary open-loop poles exist.

On the contrary, if there exist no imaginary open-loop poles, it is not hard to see that working with $\mathcal{N}_s - \epsilon$ in numerically computing the locus yields no sufficiency redundance as $\varepsilon \to 0$, noting that $\epsilon \geq 0$ always exists.

As a z-domain counterpart to Theorem 3, we have.

Theorem 4. Under the same assumptions of Theorem 3; the closed-loop system is stable if and only if for any s-domain contour $\mathcal{N}_z - \epsilon$ with $R > 0$ large sufficiently and $\gamma > 0$, $\epsilon \geq 0$ sufficiently small, any prescribed πr-sector Hurwitz polynomial $\alpha(s, r)$; the stability locus

$$g_C(z, \alpha(z,\rho))\Big|_{z\in\mathcal{N}_z-\epsilon} =: \frac{\tilde{\Delta}_G(z,\rho)\tilde{\Delta}_H(z,\rho)}{\alpha(z,\rho)} \det\left(\frac{I_m + \tilde{H}(z)\tilde{G}(z))}{\det(I_m + \Xi D)}\Big|_{z\in\mathcal{N}_z-\epsilon}\right. \tag{27}$$

satisfies: (i) $g_C(z, \alpha(z,\rho)) \neq 0$ for all $z \in \mathcal{N}_z - \epsilon$; (ii) $N\left(g_C(z, \alpha(z,\rho))\Big|_{z\in\mathcal{N}_z-\epsilon}\right) = 0$. Here, we have

$$\begin{cases} \tilde{\Delta}_G(z,\rho) = \Delta_G(s,\rho)\big|_{s^\rho=z}, \quad \tilde{\Delta}_H(z,\rho) = \Delta_H(s,\rho)\big|_{s^\rho=z} \\ \tilde{H}(z) = H(s)\big|_{s^\rho=z}, \quad \tilde{G}(z) = G(s)\big|_{s^\rho=z} \end{cases}$$

In the above, $\mathcal{N}_z - \epsilon$ is the contour by shifting $\mathcal{N}_z$ to its left with distance ϵ. Several remarks about Theorems 3 and 4:

• The shifted contour $\mathcal{N}_s - \epsilon$ reduces to the standard contour $\mathcal{N}_s$ when $\epsilon = 0$. This is also the case for the shifted contour $\mathcal{N}_z - \epsilon$ and $\mathcal{N}_z$.

• Clearly, the detouring treatments in Theorems 3 and 4 do not exist in Theorems 1 and 2, since the stability conditions in the latter ones are claimed directly on the fractional-order characteristic polynomials, in which transfer functions are not involved.

4. Numerical illustrations

4.1 Example description for Theorems 1 and 2

Consider a single fractional-order commensurate system [15] with the characteristic polynomial

$$s^{2r} + 2as^r + b = 0, \quad a, b \in \mathcal{R}$$

where the commensurate order $0 < r = \frac{k}{m} \leq 1$ with k, m, and $k \leq m$ being positive integers as appropriately. In all the numerical simulations based on Theorem 1, the fractionally commensurate Hurwitz polynomial $\beta(s,r) = (s+1)^{2r}$ is employed. In all the numerical simulations based on Theorem 2, the πr-sector Hurwitz polynomial $\alpha(z,r) = (z+0.1)^2$ is adopted.

In what follows, the s-domain contour $\mathcal{N}_s$ is defined with $\gamma = 0.01$ and $R = 100000$, while the z-domain contour $\mathcal{N}_z$ is defined with $\gamma = 0.01$ and $R = 10000$.

4.2 Numerical results for Theorems 1 and 2

The following cases are considered in terms of a and b. In each figure, the left-hand sub-figure plots the stability locus in terms of $f(s,\beta(s,r))|_{s\in\mathcal{N}_s}$, or simply the s-locus, for some fixed a and , while the right-hand sub-figure presents the stability locus in terms of $g(z,\alpha(z,r))|_{z\in\mathcal{N}_z}$, or simply the z-locus.

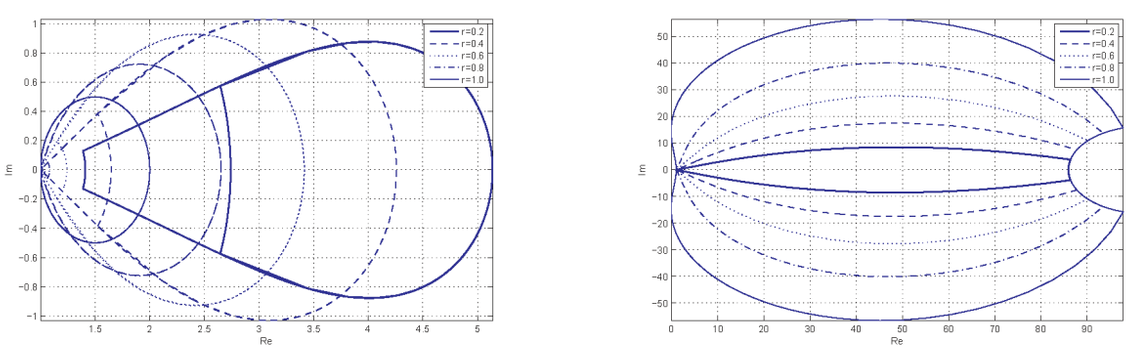

Figure 4.
Stability loci with $a = 2$ and $b = 1$.

• $a > 0$, $b > 0$, and $a^2 \geq b$. By examining the s-loci of **Figure 4** graphically, no encirclements around the origin are counted in each case of $r \in \{0.2, 0.4, 0.6, 0.8, 1.0\}$; indeed, $N\left(f(s, \beta(s,r))\Big|_{s \in \mathcal{N}_s}\right) = 0$ for each $r \in \{0.2, 0.4, 0.6, 0.8, 1.0\}$ can be verified numerically without locus plotting. Therefore, the system is stable in each case.

The same conclusions can be drawn by examining the z-loci of **Figure 4**. More precisely, we have $N\left(f(z, \alpha(z,r))\Big|_{z \in \mathcal{N}_z}\right) = 0$ for each $r \in \{0.2, 0.4, 0.6, 0.8, 1.0\}$ numerically.

• $a > 0$, $b > 0$, and $a^2 < b$. By the s-loci of **Figure 5**, no encirclements around the origin are counted in each case of $r \in \{0.2, 0.4, 0.6, 0.8, 1.0\}$ graphically; or $N\left(f\left(s, \beta(s,r)\right)\Big|_{s \in \mathcal{N}_s}\right) = 0$ for each $r \in \{0.2, 0.4, 0.6, 0.8, 1.0\}$ numerically. Therefore, the system is stable in each case.

The same conclusions can be drawn by examining the z-loci of **Figure 5**. More precisely, we have $N\left(f\left(z, \alpha(z,r)\right)\Big|_{z \in \mathcal{N}_z}\right) = 0$ for each $r \in \{0.2, 0.4, 0.6, 0.8, 1.0\}$ numerically.

• $a < 0$, $b < 0$, and thus $a^2 \geq b$ holds always. By the s-loci of **Figure 6**, one net encirclement around the origin is counted in each case of $r \in \{0.2, 0.4, 0.6, 0.8, 1.0\}$ graphically; alternatively, $\left|N\left(f\left(s, \beta(s,r)\right)\Big|_{s \in \mathcal{N}_s}\right)\right| = 1$ for each $r \in \{0.2, 0.4, 0.6, 0.8, 1.0\}$ numerically. Therefore, the system is unstable in each case.

The instability conclusions in each $r \in \{0.2, 0.4, 0.6, 0.8, 1.0\}$ can be revealed by means of the z-loci of **Figure 6**. More precisely, we have $N\left(f\left(z, \alpha(z,r)\right)\Big|_{z \in \mathcal{N}_z}\right) = 1$ for each $r \in \{0.2, 0.4, 0.6, 0.8, 1.0\}$ numerically.

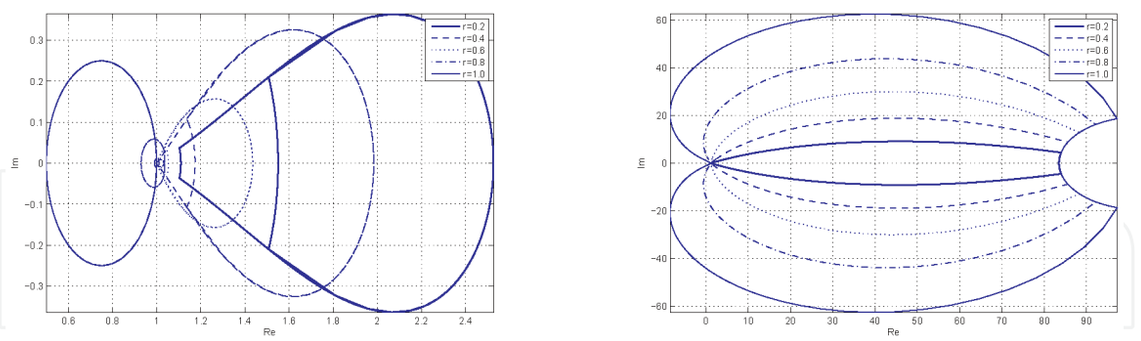

Figure 5.
Stability loci with $a = 1/2$ and $b = 1$.

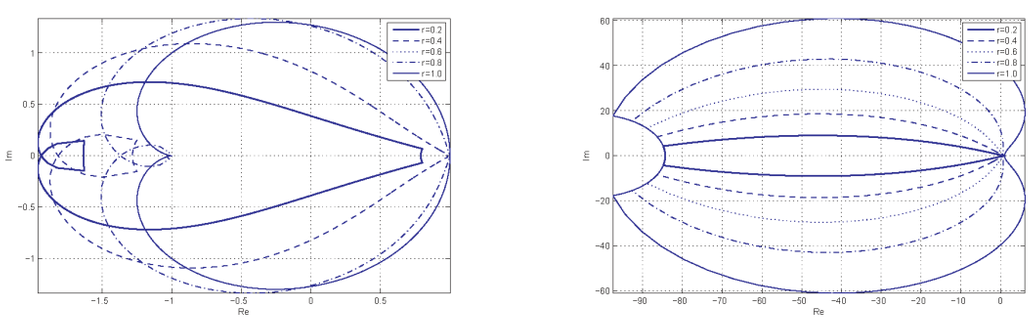

Figure 6.
Stability loci with $a = -1$ and $b = -1$.

• $a > 0$, $b < 0$, and thus $a^2 \geq b$ holds always. By the s-loci of **Figure 7**, one net encirclement around the origin is counted in each case of $r \in \{0.2, 0.4, 0.6, 0.8, 1.0\}$ graphically; alternatively, $\left|N\left(f\left(s, \beta(s,r)\right)\Big|_{s \in \mathcal{N}_s}\right)\right| = 1$ for each $r \in \{0.2, 0.4, 0.6, 0.8, 1.0\}$ numerically. Therefore, the system is unstable in each case.

The instability conclusions in each $r \in \{0.2, 0.4, 0.6, 0.8, 1.0\}$ can be drawn again by means of the z-loci of **Figure 7**. More precisely, we have $N\left(f\left(z, \alpha(z,r)\right)\Big|_{z \in \mathcal{N}_z}\right) = 1$ for each $r \in \{0.2, 0.4, 0.6, 0.8, 1.0\}$ numerically.

• $a < 0$, $b > 0$, and $a^2 \geq b$. By the s-loci of **Figure 8**, one net encirclement around the origin is counted in the case of $r = 0.2$ graphically, or $\left|N\left(f\left(s, \beta(s,r)\right)\Big|_{s \in \mathcal{N}_s}\right)\right| = 1$ for $r = 0.2$ numerically; two net encirclements around the origin are counted in each case of $r \in \{0.4, 0.6, 0.8, 1.0\}$, or $\left|N\left(f\left(s, \beta(s,r)\right)\Big|_{s \in \mathcal{N}_s}\right)\right| = 2$ for each $r \in \{0.4, 0.6, 0.8, 1.0\}$ numerically. Therefore, the system is unstable in each case of $r \in \{0.2, 0.4, 0.6, 0.8, 1.0\}$.

The instability conclusions in each $r \in \{0.2, 0.4, 0.6, 0.8, 1.0\}$ can be drawn again by means of the z-loci of **Figure 8**. More specifically, we have $N\left(f\left(z, \alpha(z,r)\right)\Big|_{z \in \mathcal{N}_z}\right) = 1$ for $r = 0.2$ and $N\left(f\left(z, \alpha(z,r)\right)\Big|_{z \in \mathcal{N}_z}\right) = 2$ for each $r \in \{0.4, 0.6, 0.8, 1.0\}$ numerically.

• $a < 0$, $b > 0$, and $a^2 < b$. By the s-loci of **Figure 9**, no encirclements around the origin are counted in each case of $r \in \{0.2, 0.4, 0.6\}$ graphically, or $\left|N\left(f\left(s, \beta(s,r)\right)\Big|_{s \in \mathcal{N}_s}\right)\right| = 0$ for each $r \in \{0.2, 0.4, 0.6\}$ numerically. Therefore, the system is stable in each case of $r \in \{0.2, 0.4, 0.6\}$. However, two net encirclements around the origin are counted in each case of $r \in \{0.8, 1.0\}$ graphically or

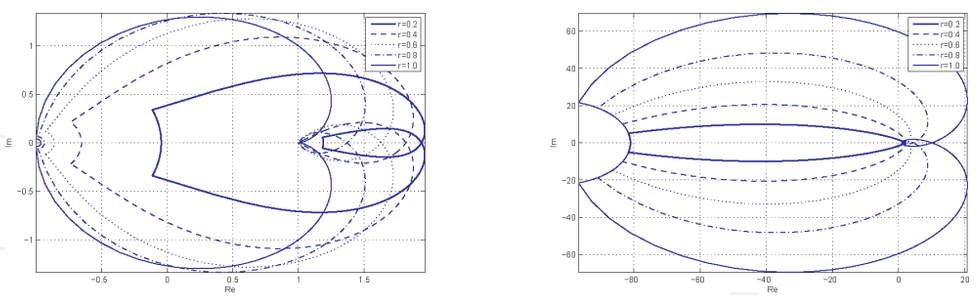

Figure 7.
Stability loci with $a = 1$ and $b = -1$.

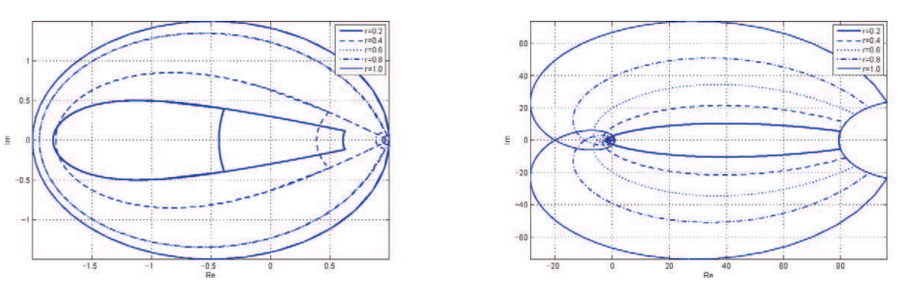

Figure 8.
Stability loci with $a = -2$ and $b = 1$.

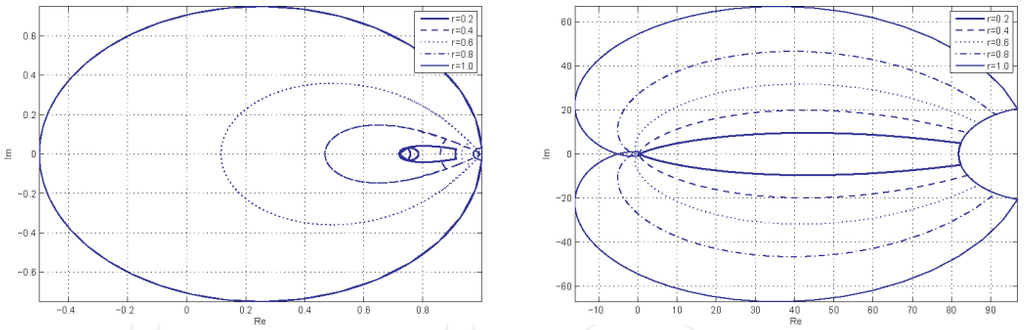

Figure 9.
Stability loci with $a = -1/2$ and $b = 1$.

	K_P	K_I	K_D	μ	λ
Case 1	1.2623	0.5531	0.2382	1.2555	1.1827
Case 2	1.2623	0.5526	0.2381	1.2559	1.1832

Table 1.
PID controller parameters.

$\left|N\left(f\left(s,\beta(s,r)\right)\Big|_{s\in\mathcal{N}_s}\right)\right| = 2$ for each $r\in\{0.8,1.0\}$ numerically. Therefore, the system is unstable in either case of $r\in\{0.8,1.0\}$.

Stability in each case of $r\in\{0.2,0.4,0.6\}$ and instability for either case of $r\in\{0.8,1.0\}$ can be verified by the z-loci of **Figure 9** as appropriately. Indeed, we have $N\left(f\left(z,\alpha(z,r)\right)\Big|_{z\in\mathcal{N}_z}\right) = 0$ for $r\in\{0.2,0.4,0.6\}$ and $N\left(f\left(z,\alpha(z,r)\right)\Big|_{z\in\mathcal{N}_z}\right) = 2$ for each $r\in\{0.8,1.0\}$ numerically.

Based on the numerical results, the stability/instability conclusions based on the s-loci completely coincide with those drawn based on the z-loci. This reflects the fact of Remark 2. These numerical results are also in accordance with those by [15] about the same example, which are summarized by working with solving polynomial roots. It is worth mentioning that polynomial roots are not always solvable in general. Fortunately, the suggested Nyquist-like criteria can be implemented graphically and numerically, independent of any polynomial root solution and inter-complex-plane transformation. Hence, the suggested technique is applicable more generally.

4.3 Example description for Theorem 3

Consider the feedback configuration of **Figure 1** used for automatic voltage regulator (AVR) in generators, which is formed by the subsystems [6]:

$$G(s) = \left(K_P + \frac{K_I}{s^\lambda + 0.0001} + \frac{100K_D s^\mu}{s^\mu + 100}\right)\frac{10}{(1+0.1s)(1+0.4s)(1+s)},\ H(s) = \frac{1}{1+0.01s}$$

where $H(s)$ is a regular-order sensor model and $G(s)$ is a cascading model consisting of a fractional-order PID in the form of $K_P + K_I/\left(s^\lambda + 0.0001\right) + 100K_D s^\mu/\left(s^\mu + 100\right)$ [1], an amplifier modeled as

[1] The fractional-order integral portion in the PID is approximated by $K_I/\left(s^\lambda + 0.0001\right)$ in order to avoid definition problem at the origin when it is in the form of K_I/s^λ.

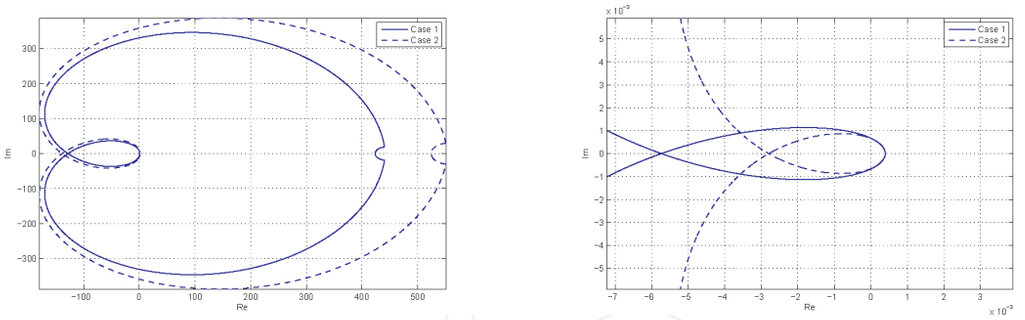

Figure 10.
Stability loci for cases 1 and 2.

$10/(1+0.1s)$, an exciter modeled as $1/(1+0.4s)$, and a generator with model $1/(1+s)$. Fractional-order PID parametrization is addressed in [6] by means of particle swarm optimization.

In the following, we focus merely on verifying the closed-loop stability based on Theorem 3, based on the parametrization results therein. To this end, the s-domain shifting contour $\mathcal{N}_s - \epsilon$ is defined with $R = 100000$, $\gamma = 0.1$, and $\varepsilon = 0.01$. To utilize Theorem 3, the fractionally commensurate Hurwitz polynomial $\beta(s,r) = (s+1)^{\lambda+\mu+4}$ is employed.

The so-called optimal controller parameters are listed in **Table 1**.

4.4 Numerical results for Theorem 3

Based on **Table 1**, the stability loci in the two cases are plotted in **Figure 10**. The stability loci for the two cases cannot be distinguished from each other graphically. By counting the outmost circle as one clockwise encirclement around the origin, then one can count another counterclockwise encirclement after zooming into the local region around the origin; it follows that the net encirclements number is zero. Indeed, our numerical phase increment computations in either case yields that $N\left(f_C\left(s,\beta(s,\rho)\right)\Big|_{s\in\mathcal{N}_s-\varepsilon}\right) = 0$. From these facts, Theorem 3 ensures that the closed-loop fractional-order system is stable. This coincides with the results in [6].

5. Conclusions

Stability is one of the imperative and thorny issues in analysis and synthesis of various types of fractional-order systems. By the literature [28–30], the frequently adopted approaches are through single/multiple complex transformation such that fractional-order characteristic polynomials are transformed into standard regular-order polynomials, and then stability testing of the concerned fractional-order systems is completed by the root distribution of the corresponding regular-order polynomials. In view of the root computation feature, such existing approaches are direct in testing methodology.

In this paper, we claimed and proved an indirect approach that is meant also in the s-complex domain but involves no root computation at all. What is more, the main results can be interpreted and implemented graphically with locus plotting as we do in the conventional Nyquist criteria, as well as numerically without any locus plotting (or simply via complex function argument integration). This implies that the complex scaling approach is numerically tractable so that is much more

applicable in fractional-order control design and parametrization. This point is significant for practical control applications involving fractional-order plants, which are our perspective topics in the future.

Acknowledgements

The study is completed under the support of the National Natural Science Foundation of China under Grant No. 61573001.

Author details

Jun Zhou
Department of Control Engineering, School of Energy and Electrical Engineering, Hohai University, Nanjing, China

*Address all correspondence to: katsura@hhu.edu.cn

References

[1] Fedele G, Ferrise A. Periodic disturbance rejection with unknown frequency and unknown plant structure. Journal of the Franklin Institute. 2014; **351**:1074-1092

[2] Fedele G, Ferrise A. Periodic disturbance rejection for fractional-order dynamical systems. Fractional Calculus and Applied Analysis. 2015; **18**(3):603-620

[3] Li MD, Li DH, Wang J, Zhao CZ. Active disturbance rejection control for fractional-order system. ISA Transactions (The Journal of Automation). 2013;**52**:365-374

[4] Padula F, Visioli A. Tunning rules for optimal PID and fractional-order PID controllers. Journal of Process Control. 2011;**21**:69-81

[5] Podlubny I, Petráš I, Vinagre BM, O'Leary P, Dorčák L. Analogue realizations of fractional-order controllers. Nonlinear Dynamics. 2002; **29**:281-296

[6] Ramezanian H, Balochian S, Zare A. Design of optimal fractional-order PID controllers using particle swarm optimization for automatic voltage regulator (AVR) system. Journal of Control, Automation and Electrical Systems. 2013;**24**:601-611

[7] Raynaud HF, Zergainoh A. State-space representation for fractional order controllers. Automatica. 2000;**36**: 1017-1021

[8] Tavazoei MS. A note on fractional-order derivatives of periodic functions. Automatica. 2010;**48**:945-948

[9] Wang JC. Realizations of generalized warburg impedance with RC ladder networks and transmission lines. Journal of the Electrochemical Society. 1987; **134**(8):1915-1920

[10] Podlubny I. Fractional-Order Differential Equations. San Diego: Academic Press; 1999

[11] Biswas K, Sen S, Dutta PK. Realization of a constant phase element and its performance study in a differentiabtor circuit. IEEE Transactions on Circuits and Systems - I. 2006;**53**(9):802-807

[12] Chen YQ. Ubiquitous fractional order controls? In: Plenary talk in the Second IFAC Symposium on Fractional Derivatives and Applications (IFAC FDA2006); Port, Portugal; 2006

[13] Chen YQ, Petráš I, Xue D. Fractional order control—A tutorial. In: Proceedings of the 2009 American Control Conference; 2009. pp. 1397-1411

[14] Alagoz BB. A note on robust stability analysis of fractional order interval systems by minimum argument vertex and edge polynomials. IEEE/CAA Journal of Automatica Sinica. 2016;**3**(4): 411-417

[15] Radwan AG, Soliman AM, Elwakil AS, Sedeek A. On the stability of linear systems with fractional-order elements. Chaos, Solitons & Fractals. 2009;**40**:2317-2328

[16] Stein EM, Shakarchi R. Complex Analysis. Princeton/Oxford: Princeton University Press; 2003. 379p

[17] Zhou J. Generalizing Nyquist criteria via conformal contours for internal stability analysis. Systems Science & Control Engineering. 2014;**2**: 444-456. DOI: 10.1080/21642583. 2014.915204

[18] Zhou J, Qian HM. Pointwise frequency responses framework for stability analysis in periodically

time-varying systems. International Journal of Systems Science. 2017;**48**(4): 715-728. DOI: 10.1080/00207721.2016.1212430

[19] Zhou J, Qian HM, Lu XB. An argument-principle-based framework for structural and spectral characteristics in linear dynamical systems. International Journal of Control. 2017;**90**(12):2598-2604. DOI: 10.1080/00207179.2016.1260163

[20] Zhou J, Qian HM. Stability analysis of sampled-data systems via open/closed-loop characteristic polynomials contraposition. International Journal of Systems Science. 2017;**48**(9):1941-1953. DOI: 10.1080/00207721.2017.1290298

[21] Zhou J. Complex scaling circle criteria for Lur'e systems. International Journal of Control. 2019;**92**(5):975-986. DOI: 10.1080/00207179.2017.1378439

[22] Zhou J. Interpreting Popov criteria in Lure systems with complex scaling stability analysis. Communications in Nonlinear Science and Numerical Simulation. 2018;**59**:306-318. DOI: 10.1016/j.cnsns.2017.11.029

[23] Zhou J, Gao KT, Lu XB, et al. Mathematical Problems in Engineering. 2018;**2018**:8492735. DOI: 10.1155/2018/8492735. 14p

[24] Zhou J, Gao KT, Lu XB. Stability analysis for complicated sampled-data systems via descriptor remodeling. IMA Journal of Mathematical Control and Information. 2018. DOI: 10.1093/imamci/dny031

[25] Zhou J. Stability analysis and stabilization of linear continuous-time periodic systems by complex scaling. International Journal of Control. 2018. DOI: 10.1080/00207179.2018.1540888

[26] Zhou J. Complex-domain stability criteria for fractional-order linear dynamical systems. IET Control Theory and Applications. 2017;**11**(16): 2753-2760. DOI: 10.1049/iet-cta.2016.1578

[27] Watanabe R, Miyazaki H, Ehto S. Complex Analysis. Tokyo: Pefukan Press; 1991

[28] Monje CA, Chen YQ, Vinagre BM, Xue DY, Feliu V. Fractional-Order Systems and Controls: Fundamentals and Applications. London/New York: Springer; 2010

[29] Rajas-Moreno A. An approach to design MIMO fractional-order controllers for unstable nonlinear systems. IEEE/CAA Journal of Automatica Sinica. 2016;**3**(3):338-344

[30] Soorki MN, Tavazoei MS. Constrained swarm stabilization of fractional order linear time invariant swarm systems. IEEE/CAA Journal of Automatica Sinica. 2016;**3**(3):320-331